Hysteresis Loss in Filled Rubber Vulcanizates and Its Relationship with Heat Generation

KAMAL K. KAR, ANIL K. BHOWMICK

Rubber Technology Centre, Indian Institute of Technology, Kharagpur, 721 302, India

Received 7 June 1996; accepted 14 August 1996

ABSTRACT: A relationship between heat generation of filled rubber vulcanizates and hysteresis loss, specific heat, thermal conductivity, modulus, filler loading, structure, and surface area of the filler, the temperature difference between application temperature and glass transition temperature, frequency, temperature difference between the wall and the environment, stress, and stroke amplitude were developed. Styrene–butadiene rubber (SBR) and natural rubber (NR) vulcanizates were used that had variations of loading of carbon black, silica, resin and coupling agent, types of filler, level of curatives, and cure time. The derived equation was verified with a set of a few unknown SBR and NR vulcanizates, and also by varying the stress and stroke amplitudes in the heat generation experiment. © 1997 John Wiley & Sons, Inc. J Appl Polym Sci **64:** 1541–1555, 1997

Key words: hysteresis; rubber vulcanizates; heat generation

INTRODUCTION

During deformation of rubber, a part of the mechanical energy is converted into heat and other forms of energy. The loss of mechanical energy is the hysteresis loss. The mechanism of hysteresis loss in a rubber compound is still obscure, although many properties like traction, wear, modulus, heat generation, tear, etc., are often correlated with the hysteresis in the literature. However, it has been amply demonstrated that the energy loss in the compound plays a key role in better performance, particularly in applications where an elastomer is subjected to repeated deformation of sufficient magnitude and frequency, as in the case of airplane and truck tires and rubberized road wheels used in the battle tank. The reports[1] on failure analysis of these products reveal that the rubber failure is attributed to one or a combination of all of the following mechanisms: high heat buildup, blowout, chipping and chunking, cracking due to surface embrittlement by thermal oxidation and ozone attack, mechanochemical decomposition due to very high frictional work, and hysteresis loss on vehicle suffling. In spite of its obvious importance there is surprisingly little published work dealing with the quantitative relationship between hysteresis loss and heat generation in rubber compounds.

Actually heat generation in rubber is determined by the nature of the polymers, the physical and chemical properties of the compounding ingredients, and their interaction with rubber, operating parameters, and the working environments. Out of the three products mentioned above, the heat generation of road wheel rubber compounds has not been studied at all. Most of the studies on heat generation have been done on pneumatic tires.[2] In most cases the characteristics of these compounds are low hardness with low heat buildup. But the road wheel compounds have high hardness and demand low heat buildup. Various aspects of the dynamic properties of polymers, viscoelasticity of rubber components, the molecular frictional coefficients, and their depen-

Correspondence to: A. K. Bhowmick.

dence on temperature were reported[3] and an attempt was made to explain the heat generation of simple polymeric materials under very low strain amplitude. It was observed that the temperature reached after lengthy running of tires depends on the ratio of heat generation and heat dissipation. The energy loss per cycle during sinusoidal deformation may be given as follows:

$$E' = \pi(\gamma_o)^2 G''(\omega) \quad (1)$$

at constant strain[4]

$$E' = \pi(\sigma_o)^2 J''(\omega) \quad (2)$$

at constant stress[5] and

$$E_{\text{loss1}}/E_{\text{loss2}} = \tan \delta_1/\tan \delta_2 \quad (3)$$

at constant energy,[6] where δ_1 and δ_2 are phase angles; E', E_{loss1}, and E_{loss2} are energy losses per cycle; γ_o is the strain amplitude; σ_o is the stress amplitude; $G''(\omega)$ is the loss modulus; and $J''(\omega)$ is the loss compliance. Steady-state temperature rise (ΔT) for some compounds in continuous cyclic deformation (measured in a Goodrich flexometer), taking into account nonlinearity of response and the effect of added filler in a rubbery polymer, was given by[3]

$$\Delta T = c(1 - bv)[\omega \gamma_0^2 E''(W, T_1)/2] \quad (4)$$

where W is the radian frequency of deformation, T_1 is the steady-state temperature, v is the volume fraction of filler, and the coefficients c and b are 1.1 E-06 deg cm^3 s erg^{-1} and 2.4, respectively.

Priss[7] showed that the relative mechanical loss per wheel rotation could be calculated from the dynamic properties determined under sinusoidal load for any deformation. The effect of carbon black loading and crosslink density on the heat build-up in the elastomer was recently discussed by Meinecke.[8] Medalia[9] reviewed the viscoelastic properties of carbon black and silica filled rubbers on heat generation. Gent and Hindi[10] performed an excellent experiment on the blow out phenomena in rubber and correlated blowing out of rubber with the voids and the elastic modulus of rubber by using

$$T_m = T_o + Q'H^2/8K'' \quad (5)$$

where K'' is the coefficient of thermal conductivity of the material, T_m is the maximum temperature at the central plane, H is the thickness, Q' is the heating rate (J/m^3 s), and T_o is the surface temperature.

Heat generation in a rubber compound is not an intrinsic material property; rather it depends on the physical properties of rubber and/or operating variables. Therefore, a reliable relationship between heat generation of rubbers and both the operating variables and the polymer material properties is desirable to obtain a better understanding of the heat generation behavior. In this study we investigated the effect of various compounding ingredients on heat generation and hysteresis loss. Finally, a model was developed by using dimensional analysis to understand the dependence of heat generation on hysteresis loss and other parameters.

Our research work was carried out in eight phases, as follows:

1. study of styrene–butadiene rubber (SBR) based compounds with variation of carbon black loading;
2. study of compounds based on natural rubber (NR) with variation of carbon black loading;
3. study of compounds based on NR with variation of resin loading;
4. study of compounds based on NR with variation of loading of silica filler and coupling agent;
5. study of compounds based on NR with variation of type of black;
6. study of compounds based on NR with variation of curative loading;
7. study of NR based compounds having various cure times; and
8. study of NR based compounds containing black, silica, and resin, a formulation similar to road wheel rubber compounds.

EXPERIMENTAL

Materials and Formulations

The formulations of the various mixes are given in Table I. They are designated as A_i, B_i, C_i, D_i, E_i, F_i, G_i, and H_i corresponding to phases 1–8. The subscript i may vary as 0, 20, 30, 40, 50, 60, and 70 parts by weight, which may be loading of carbon black, resin, or silica. NR (RMA4), SBR-

Table I Formulation of Phases 1–8 in PHR

Mix Number	A_i	B_i	C_i	D_i	E_i	F_i	G_i	H_i
NR	0	100	100	100	100	100	100	100
SBR	100	0	0	0	0	0	0	0
ZnO	5.0	5.0	5.0	5.0	5.0	5.0	5.0	5.0
Stearic acid	2.0	2.0	2.0	2.0	2.0	2.0	2.0	2.0
TMQ	1.5	1.5	1.5	1.5	1.5	1.5	1.5	1.5
6PPD	1.5	1.5	1.5	1.5	1.5	1.5	1.5	1.5
ISAF black	$A_{i=0-70}$	$B_{i=0-70}$	$C_{i=0-50}$	$D_{i=0-50}$	50	50	50	50
Other black	0	0	0	0	$E_{i=1-3}$	0	0	10.0
Silica	0	0	0	$D_{i=0-50}^{j=0-20}$	0	0	0	10.0
Aromatic oil	5.0	5.0	5.0	5.0	5.0	5.0	5.0	5.0
Si-69	0	0	0	2.5	0	0	0	0
Resin	0	0	$C_{i=0-50}^{j=0-30}$	0	0	0	10.0	0
BSM	0.8	0.8	0.8	0.8	0.8	$F_{i=1-6}$	0.8	0.8
Sulfur	2.5	2.5	2.5	2.5	2.5	$F_{i=1-6}$	2.5	2.5
PVI	0.5	0.5	0.5	0.5	0.5	0.5	0.5	0.5

A_i = 0–70: A_0, A_{20}, A_{30}, A_{40}, A_{50}, A_{60}, and A_{70}; subscript indicates loading of filler.
B_i = 0–70: B_0, B_{20}, B_{30}, B_{40}, B_{50}, B_{60}, and B_{70}.
$C_{i=0-50}^{j=0-30}$: C_0^0, C_0^{10}, C_0^{20}, C_0^{30}, C_{50}^0, C_{50}^{10}, and C_{50}^{20} (j indicates resin loading).
$D_{i=0-50}^{j=0-20}$: D_0^0, D_0^{10}, D_0^{20}, $D_0^{20+2.5\text{phr Si-69}}$, D_{50}^0, D_{50}^{10}, and $D_{50+2.5\text{phr Si-69}}^{20}$ (j indicates silica loading).
E_i = 1–3: E_1 (10 phr HAF), E_2 (10 phr GPF), and E_3 (10 phr Vulcan-xc-72).
F_i = 1–6: F_1 (BSM/S = 0.8/2.5), F_2 (BSM/S = 1.5/1.5), F_3 (BSM/S = 1.0/1.0), F_4 (BSM/S = 3/3), F_5 (BSM/S = 2.0/2.0), and F_6 (BSM/S = 2.5/2.5).
G_i = Cure at t_{90}, t_{90+10}, and t_{90+20} for tensile samples. Cure at t_{90+10}, t_{90+30}, t_{90+60} for heat buildup specimens.

1502, stearic acid, Si-69 (Degussa A.G), and aromatic oil were supplied by Birla Tyres Ltd., Balasore. ISAF (N220), HAF (N330), and GPF (N660) were supplied by Philips Carbon Black Ltd., Durgapur. Vulcan-xc-72 (N472) was obtained from Cabot Corporation, Boston. Zinc oxide was obtained from the local market. Resin (high styrene resin) and sulfur were supplied by Bengal Waterproof Ltd., Panihati. TMQ (polymerized 1,2-dihydro-2,2,4-trimethylquinoline), 6PPD [(*N*-1,3-dimethyl butyl)-*N*′-phenyl-*p*-phenylenediamine], PVI (*N*-cyclohexyl thiophthalimide), and BSM [(2-(4-morpholinyl mercapto)benzthiazole] were supplied by ICI Ltd., Rishra.

Mixing

The compounding ingredients were mixed with rubber on a two roll Schwabenthan mill (6 × 13 in.) supplied by Baujahr, Germany. Only the formulations containing silica and Si-69 were mixed in a Brabender Plasticorder (PLE-330) at a temperature of 140°C and a rotor speed of 60 rpm with the mixing specifications given in Table II.

Final mixing of sulfur, accelerator, and retarder was done in the same laboratory two roll mill. The temperature of mixing was kept below 50°C.

Curing

The curing characteristics of the mixes were evaluated with a rheometer R-100 according to ASTM D 2084-81. Subsequent moldings were carried out in a David Bridge press (supplied by Castleten Rocchdle, England) at a temperature of 150°C, pressure of 4 MPa, and optimum cure time (t_{90}) for tensile specimens and t_{90} + 10 min for heat buildup specimens.

Table II Mixing Specifications

Time (min)	Temperature (°C)	Mixing of Ingredients
0	140	Addition of rubber
1	140	Addition of all chemical ingredients except aromatic oil
4	140	Aromatic process oil
5	150	Discharge

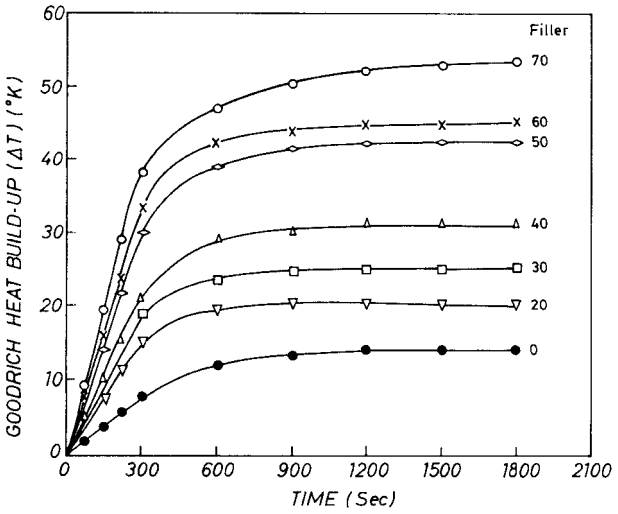

Figure 1 Effect of dynamic compression time on Goodrich heat buildup at a temperature of 50°C, a stroke amplitude of 4.45 E-03 m, and stress of 0.999 MPa for NR vulcanizates; (●) gum, (▽) 20 phr ISAF, (□) 30 phr ISAF, (△) 40 phr ISAF, (◇) 50 phr ISAF, (×) 60 phr ISAF, and (○) 70 phr ISAF.

Measurements

Stress–Strain Properties

Modulus at 100% elongation, tensile strength, and elongation at break were measured at 32 and 50°C at a rate of 8.333 E-03 m/s in a Zwick UTM model 1445 according to ASTM D 412-80. Young's modulus was measured from the initial slope (below 50% elongation) of the stress–strain curves for all samples.

Heat Buildup Measurement and Calculation of Heat Generation

Heat buildup was measured by a Goodrich flexometer according to ASTM D 623-81 at 32 and 50°C at various strokes (4.45, 6.0, and 8.0 mm) and at various loads (724, 999, 1303, and 1905 kPa). Cylindrical rubber specimens, 25 mm high and 17.5 mm in diameter, were used. The frequency of measurement was 1800 cycles/min. The rate of temperature rise was calculated from the initial slope of the plot of temperature rise versus time (shown in Fig. 1).

The rate of heat generation per unit volume was calculated from the calorimetry equation

$$q = mC_p d\theta/dt \qquad (6)$$

where m is the mass of the sample, C_p is the specific heat of the material at the desired temperature, and $d\theta/dt$ is the rate of temperature rise (calculation from Fig. 1).

Hysteresis Loss Under Extension

Hysteresis loss up to 100% extension was measured on a Zwick UTM (model 1445) equipped with an environmental chamber according to ASTM D 412-80. The samples were mounted in mechanical clamps 44 mm apart and the crosshead was adjusted to give zero tension. The temperature range was 32–50°C and the crosshead speed was 8.333 E-03 m/s. The temperature was controlled to ±0.5°C. The samples were preconditioned in a Zwick heating chamber for 10 min before testing. These data were used to verify the validity of the conventional theory that the heat build-up in a rubber compound is proportional to the hysteresis loss over a range of compositions.

Hysteresis Loss Under Compression

To correlate the heat buildup with hysteresis loss, hysteresis loss was determined under compression. The dimensions of the sample were the same as the Goodrich heat buildup sample. The top and bottom surfaces of the specimens were glued to metal plates to arrest slippage and uneven compression of the sample during the experiment. The samples were preconditioned in the same Zwick heating chamber for 30 min at the experimental temperature. The samples were placed in between two clamps and the crossheads were adjusted to give zero tension. The samples were precompressed up to 240 N at a crosshead speed of 8.33 E-05 m/s and then further compressed to 4.45 E-03 m at a crosshead speed between 8.33 E-05 m/s and 4.166 E-03 m/s in each cycle. Hysteresis loss was measured up to 30 cycles and it was noted that there was no significant change of hysteresis loss after this cycle. An attempt was made to measure hysteresis loss under similar conditions to the Goodrich heat buildup experiments. For the purpose of obtaining hysteresis energy loss continuously, the stress–strain curves over a range of temperatures and rates were recorded on tape and fed into a computer. Hysteresis (Hy) loss was calculated as

$$\mathrm{Hy} = \mathrm{Hy}_1 + \mathrm{Hy}_2 + \mathrm{Hy}_3 + \cdots + \mathrm{Hy}_{30} \qquad (7)$$

Here the subscript indicates the number of cycles.

Because 30 cycles were completed in 1 s, the values corresponded to hysteresis loss per second. These data were transformed to the frequency of

deformation (30 Hz) used during Goodrich heat buildup experiments with the help of the universal Williams–Landel–Ferry (WLF) rate temperature shift factor $\log a_t^3$.

$$\log a_t = -17.44(T' - T_g)/(51.6 + T' - T_g) \quad (8)$$

where T_g is the glass transition temperature and T' is the experimental temperature. The data on hysteresis loss under compression was used to derive the model equation.

Glass Transition Temperature

For the measurement of the glass transition temperature and tan δ of rubber vulcanizates, a dynamic mechanical thermal analyzer (DMTA, Rheometric Scientific, MK-II) was used at 30 Hz over a range of temperatures from −120 to 150°C and at a peak to peak displacement of 64 μm with a heating rate of 2°C/min under shear mode.

Specific Heat

Specific heat was measured by DSC (Stanton Redcroft STA 780 series) from 20 to 200°C in air with a heating rate of 5°C/min.

Thermal Conductivity

The values of thermal conductivity were taken from the literature.[11,12]

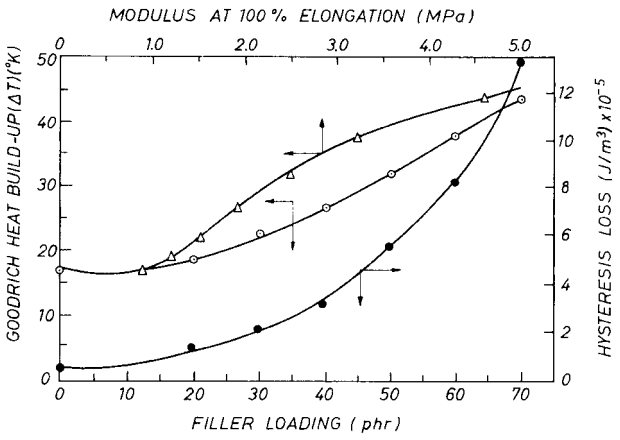

Figure 2 (a) Effect of carbon black loading and modulus on Goodrich heat buildup. (b) Effect of carbon black loading on hysteresis loss of SBR samples. Measurements were done under standard ASTM conditions. Heat buildup was measured at a stroke amplitude of 4.45 E-03 m and stress of 0.999 MPa. The modulus at 100% elongation was measured at 32°C and hysteresis loss was measured at 32°C at an extension of 100% and at a crosshead speed of 8.33 E-03 m/s.

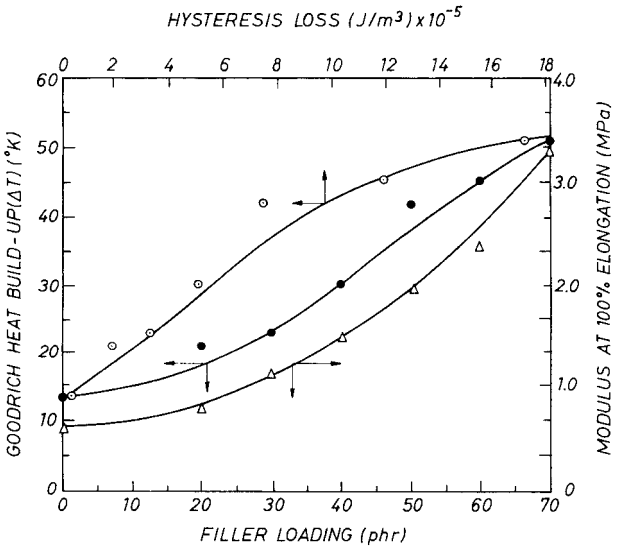

Figure 3 (a) Effect of carbon black loading and hysteresis loss on Goodrich heat buildup. (b) Effect of carbon black loading on modulus of NR vulcanizates. Measurements were carried out under the same experimental conditions as given in Figure 2.

RESULTS AND DISCUSSION

The values of Goodrich heat buildup are plotted against time in Figure 1 for different samples. The temperature increases with time for all the samples until a plateau is reached. As expected, the gum vulcanizates show lower temperature generation than the filled compounds. The higher the carbon black loading, the higher the temperature developed due to more breakage of the carbon black structure and viscoelastic losses. Hysteresis, heat buildup, and modulus of the various formulations are shown in Figures 2–8. Figures 2 and 3 reveal that the heat buildup of filled SBR and NR compounds (phases 1 and 2, Table I) increases either with increasing hysteresis, modulus, or loading of carbon black filler, although the proportionality is not linear. This may be due to the disproportionate breaking and reformation of the interaggregate bonds of carbon black as proposed by Medalia.[9] The results of the phase 4 study shown in Figure 4 displays a normal trend in agreement with Wagner's and Wolff's observations.[13–15] However, the results of phase 7 (i.e., the variations of extended curing on heat buildup and hysteresis) indicate a marginal increase of these properties with cure time (Fig. 5). The heat buildup increases without changing hysteresis in resin filled gum-NR compounds of phase 3 (Fig. 6). In filled compounds the heat buildup de-

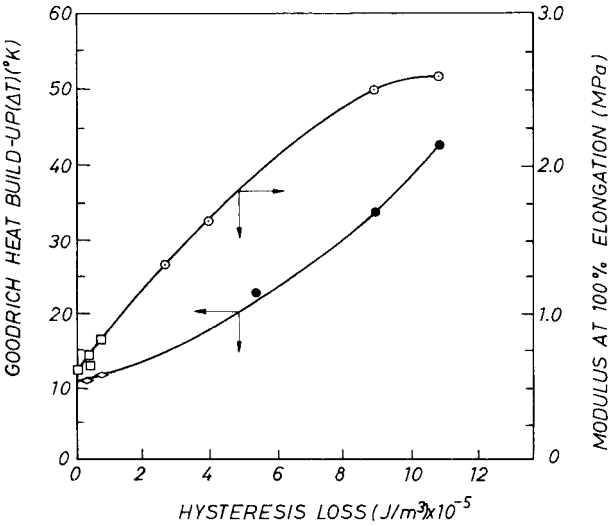

Figure 4 Effect of hysteresis loss on Goodrich heat buildup and modulus of silica, black, and Si-69 filled NR vulcanizates (mixes $D_{i=0-50}^{j'=0-20}$) measured under the same experimental conditions as given in Figure 2: (□, ◇) gum and (⊙, ●) black filled.

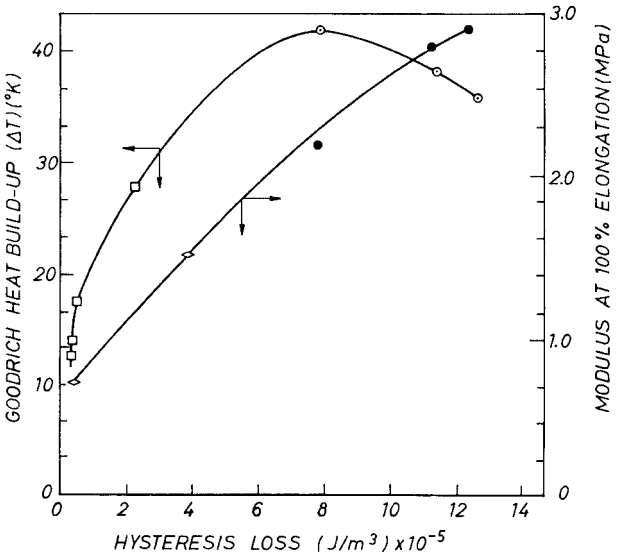

Figure 6 Effect of hysteresis loss on Goodrich heat buildup and modulus of resin filled NR vulcanizates (mixes $C_{i=0-50}^{j=0-30}$) measured under the same experimental conditions as given in Figure 2: (□, ◇) gum and (⊙, ●) black filled.

creases with hysteresis. The heat buildup, however, increases with the increase in resin loading. The modulus in systems containing resin increases with hysteresis as expected. These results on heat buildup and hysteresis are certainly not in agreement with the conventional theory that the heat buildup in a rubber compound is proportional to the hysteresis loss. All the results of the phase 6 study at higher loading of sulfur and accelerator for a semiefficient vulcanization (semi-EV) system are also at variance (Fig. 7). Low heat buildup and at the same time higher hysteresis may be due to the higher crosslinking density. Varying the type of black at constant modulus

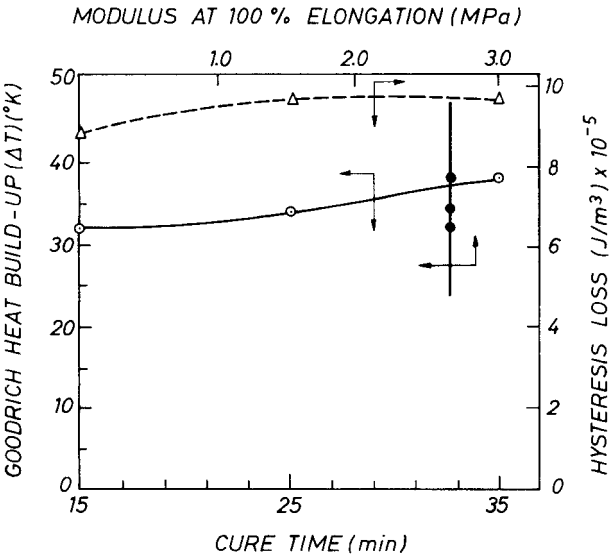

Figure 5 (a) Effect of cure time on Goodrich heat buildup and hysteresis loss. (b) Effect of modulus on Goodrich heat buildup of NR vulcanizates (mixes G_i) measured under the same experimental conditions as given in Figure 2.

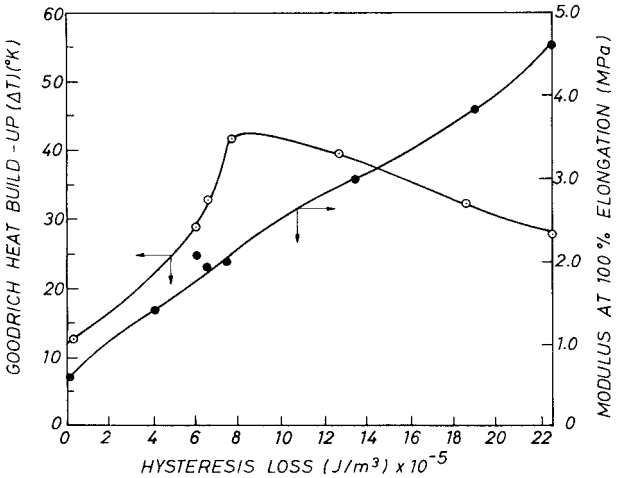

Figure 7 Effect of hysteresis loss on Goodrich heat buildup and modulus of NR vulcanizates having variations of the ratio of sulfur and accelerator (mixes $F_{i=1-6}$) measured under the same experimental conditions as given in Figure 2.

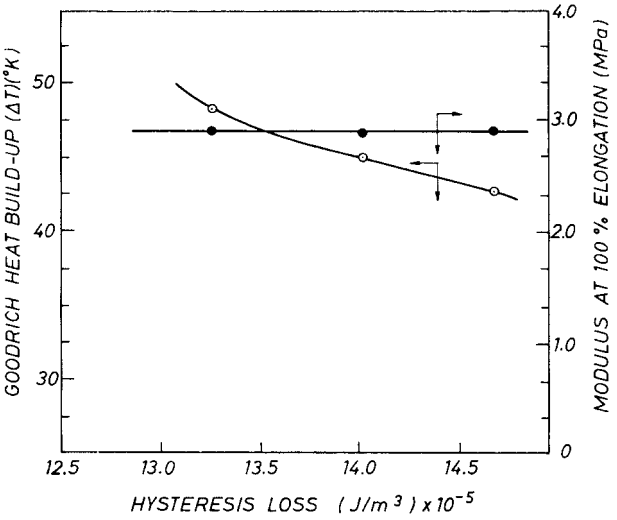

Figure 8 Effect of hysteresis loss on Goodrich heat buildup and modulus of filled NR vulcanizates having various types of black (mixes $E_{i=1-3}$) measured under the same experimental conditions as given in Figure 2.

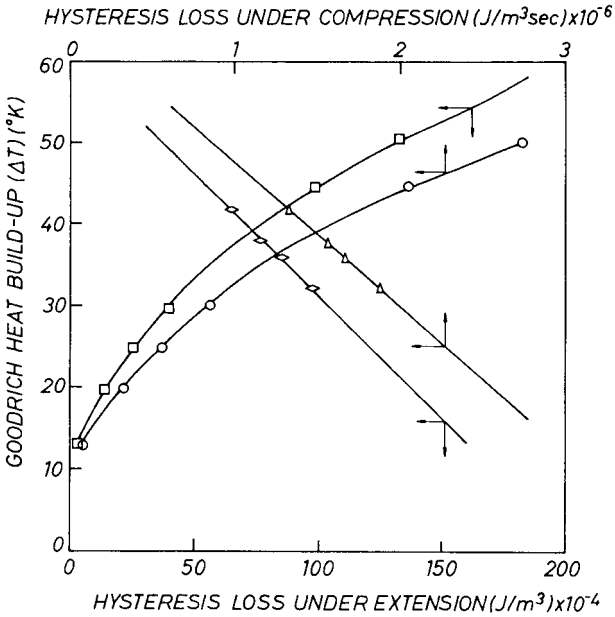

Figure 9 Effect of hysteresis loss on Goodrich heat buildup of NR vulcanizates with variation of black loading (mixes $B_{i=0-70}$) and resin loading in black filled mixes (mixes $C_{50}^{i=0-20}$). Hysteresis loss was measured under extension (at 50°C, at 100% extension, and crosshead speed of 8.33 E-03 m/s) and compression (at 50°C, preload of 240 N, compression of 4.45 E-03 m). The data were converted to 30 Hz by using the universal WLF equation.[3]

and at constant loading of carbon black, the heat buildup increases with decreasing hysteresis as shown in Figure 8. This may be due to the change of thermal conductivity and specific heat. The trends in the results of heat buildup and hysteresis loss under extension, as discussed earlier, were also true when the measurements were carried out under compression. For example, Figure 9 shows the variation of Goodrich heat buildup with hysteresis loss for filled compounds. The trends are exactly similar. The above results clearly point out that the heat buildup is a complicated function of the hysteresis loss. Although in certain vulcanizates a proportionality between these two quantities is observed, factors in addition to hysteresis predominate in deciding the heat buildup of other rubber compounds. The question is what these factors are and how they are correlated.

Development of Model Equation for Heat Generation of Rubber

From the above discussion it is difficult to draw any conclusion on the contributing factors. An attempt was made to develop a model equation for heat generation by using dimensional analysis. Dimensional analysis is based on the hypothesis that the solution of the problem is expressible by means of a dimensionally homogeneous equation of specified variables. Bhowmick et al.[16] used dimensional analysis earlier to study band formation behavior on a two roll mill, while Kar and Bahadur[17] and Viswanath and Below[18] used this approach for understanding wear of polymers. The principles and methods of dimensional analysis are given in several textbooks.[19–21] The heat generation is a function of several parameters, which are listed in Table III with their dimension. Here Q is the heat, M is the mass, L is the length, F is the force, θ is the temperature, and T is the time.

Let us apply the Buckingham π method of dimensional analysis to find out the dimensionless groups and to reduce the number of variables. We may write

$$\phi[q,\ (T' - T_g),\ \nu,\ \text{SA},\ C_p,\ \lambda,\ \text{Hy},\ \text{St},\ \text{Sa},\ M_o,\ F',\ \Delta T,\ S] = 0 \quad (9)$$

where ϕ is some arbitrary function. Let us choose $QFMT\theta L$ as primary functions. As six dimensions are involved, six repeating variables have to be selected that must contain all six dimensions. We choose $(T' - T_g)$, ν, SA, λ, C_p, and S as the vari-

ables. Therefore, there must be seven π parameters:

$$\pi_1 = (T' - T_g)^{a1}(\nu)^{b1}(\mathrm{SA})^{c1}(\lambda)^{d1}(C_p)^{e1}(S)^{f1}q$$
$$\pi_2 = (T' - T_g)^{a2}(\nu)^{b2}(\mathrm{SA})^{c2}(\lambda)^{d2}(C_p)^{e2}(S)^{f2}\mathrm{Hy}$$
$$\pi_3 = (T' - T_g)^{a3}(\nu)^{b3}(\mathrm{SA})^{c3}(\lambda)^{d3}(C_p)^{e3}(S)^{f3}\mathrm{St}$$
$$\pi_4 = (T' - T_g)^{a4}(\nu)^{b4}(\mathrm{SA})^{c4}(\lambda)^{d4}(C_p)^{e4}(S)^{f4}\mathrm{Sa}$$
$$\pi_5 = (T' - T_g)^{a5}(\nu)^{b5}(\mathrm{SA})^{c5}(\lambda)^{d5}(C_p)^{e5}(S)^{f5}M_o$$
$$\pi_6 = (T' - T_g)^{a6}(\nu)^{b6}(\mathrm{SA})^{c6}(\lambda)^{d6}(C_p)^{e6}(S)^{f6}F'$$
$$\pi_7 = (T' - T_g)^{a7}(\nu)^{b7}(\mathrm{SA})^{c7}(\lambda)^{d7}(C_p)^{e7}(S)^{f7}\Delta T \quad (10)$$

By expanding the π quantities into dimensions and solving, we obtain

$$\pi_1 = \frac{(\mathrm{SA})^2 q}{(T' - T_g)\lambda}, \quad \pi_2 = \frac{(\mathrm{SA})^2 \mathrm{Hy}}{(T' - T_g)\lambda}$$
$$\pi_3 = \frac{\mathrm{St}\lambda}{C_p \nu (\mathrm{SA})^2}, \quad \pi_4 = \frac{\lambda \mathrm{Sa}}{C_p (\mathrm{SA})\,\nu}, \quad \pi_5 = \frac{M_o}{S}$$
$$\pi_6 = \frac{F' C_p \nu}{\lambda(\mathrm{SA})}, \quad \pi_7 = \frac{\Delta T}{(T' - T_g)}$$
$$\phi\left[\frac{(\mathrm{SA})^2 q}{(T' - T_g)\lambda}, \quad \frac{(\mathrm{SA})^2 \mathrm{Hy}}{(T' - T_g)\lambda}, \quad \frac{\lambda \mathrm{St}}{C_p \nu (\mathrm{SA})^2}, \right.$$
$$\left. \frac{\lambda \mathrm{Sa}}{C_p \nu (\mathrm{SA})}, \quad \frac{M_o}{S}, \quad \frac{F' C_p \nu}{(\mathrm{SA})\lambda}, \quad \frac{\Delta T}{(T' - T_g)}\right] = 0. \quad (11)$$

Now inversion of π_5 and π_2, reciprocal of π_1, π_2 and π_6, π_2, and multiplication of π_4, π_6 and π_3, π_6 reduce the variables to

$$\phi\left[\frac{q}{\mathrm{Hy}}, \quad \frac{\nu(T' - T_g) C_p F'}{(\mathrm{SA})^3 \mathrm{Hy}}, \quad \frac{\lambda(T' - T_g)}{(\mathrm{SA})^2 \mathrm{Hy}}, \right.$$
$$\left. \frac{\mathrm{St}F'}{(\mathrm{SA})^3}, \quad \frac{F'\mathrm{Sa}}{(\mathrm{SA})^2}, \quad \frac{\Delta T}{(T' - T_g)}, \quad \frac{S}{M_o}\right] = 0 \quad (12)$$

The main dependent group $\{q/\mathrm{Hy}\}$ may be expressed in terms of the undetermined function ϕ comprising the other six groups. Hence, eq. (12) may be reduced to

$$\frac{q}{\mathrm{Hy}} = \phi\left[\frac{(T' - T_g)\lambda}{\mathrm{Hy}(\mathrm{SA})^2}, \quad \frac{\nu(T' - T_g) C_p F'}{\mathrm{Hy}(\mathrm{SA})^3}, \right.$$
$$\left. \frac{F'(\mathrm{Sa})}{(\mathrm{SA})^2}, \quad \frac{\mathrm{St}F'}{(\mathrm{SA})^3}, \quad \frac{\Delta T}{(T' - T_g)}, \quad \frac{S}{M_o}\right] \quad (13)$$

For a more general nonlinear relationship, eq. (13) may be rewritten with exponents a, b, c, d, e, and f for the dimensionless groups as follows:

$$\frac{q}{\mathrm{Hy}} \propto \left[\frac{(T' - T_g)\lambda}{\mathrm{Hy}(\mathrm{SA})^2}\right]^a \left[\frac{(T' - T_g) C_p F' \nu}{\mathrm{Hy}(\mathrm{SA})^3}\right]^b$$
$$\times \left[\frac{F'(\mathrm{Sa})}{(\mathrm{SA})^2}\right]^c \left[\frac{\mathrm{St}F'}{(\mathrm{SA})^3}\right]^d \left[\frac{\Delta T}{(T' - T_g)}\right]^e \left[\frac{S}{M_o}\right]^f \quad (14)$$

Table III List of Parameters with Symbols and Dimensions

Parameters	Symbol	Dimension
1. Heat generation per unit time per unit area	q	$QL^{-3}T^{-1}$
2. Temp. difference between operating temp. (T') and glass transition temp. (T_g)	$T' - T_g$	θ
3. Frequency	ν	T^{-1}
4. Stroke amplitude	SA	L
5. Specific heat of rubber	C_p	$QM^{-1}\theta^{-1}$
6. Hysteresis loss	Hy	$QL^{-3}T^{-1}$
7. Thermal conductivity of rubber	λ	$QL^{-1}\theta^{-1}T^{-1}$
8. Structure of carbon black	St	L^3M^{-1}
9. Surface area of carbon black	Sa	L^2M^{-1}
10. Young's modulus	M_o	FL^{-2}
11. Weight of carbon black in rubber	F'	M
12. Temp. difference between wall and environment	ΔT	θ
13. Stress, i.e., load per unit area	S	FL^{-2}

Table IV Physical Properties of SBR Compounds

Properties/ Mix Number	A_0	A_{20}	A_{30}	A_{40}	A_{50}	A_{60}	A_{70}
Hysteresis loss at (J m^3 s)E-06							
32°C	0.15	0.38	0.58	0.85	1.55	2.26	3.94
50°C	0.12	0.30	0.44	0.65	1.16	1.73	2.80
Young's modulus at (MPa)							
32°C	1.87	2.78	2.83	4.00	4.78	6.28	10.0
50°C	1.63	2.22	2.67	3.22	4.44	5.55	7.22
Rate of temperature rise at (K/s)							
32°C	0.04	0.07	0.08	0.10	0.12	0.14	0.16
50°C	0.06	0.05	0.06	0.07	0.09	0.11	0.12
Thermal conductivity at 32°C and 50°C (W m^{-1} K^{-1})	0.175	0.222	0.240	0.250	0.250	0.255	0.257
Specific heat at (J kg K)							
32°C	2552	2794	2697	2631	2363	2304	1808
50°C	2595	2850	2773	2683	2565	2444	1802
$(T' - T_g)$ (K) at							
32°C	51	49	49	49	48	48	48
50°C	69	67	67	67	66	66	66

Structure of the filler: 144 cm^3 dibutyl phthalate absorption/100 g; surface area of the filler: 120 m^2 N_2/g; stress on the sample during measurement of heat generation: 0.999 MPa; stroke, i.e., amplitude of deformation: 4.45 E-03 m; temperature difference between wall and environment: 1 K; frequency during measurement of heat generation: 30 Hz; cross-sectional area of the heat build-up sample: 2.488 E-04 m^2. Hysteresis loss was measured under compression and converted to 30 Hz by using the universal WLF equation.[3]

Equation (14) may be simplified and the rate of heat generation may be written with K as a proportionality constant defined as the dimensionless heat generation coefficient.

$$\frac{q}{\mathrm{Hy}} = K\left[\frac{(T' - T_g)\lambda}{\mathrm{Hy(SA)}^2}\right]^a\left[\frac{(T' - T_g)C_pF'\nu}{\mathrm{Hy(SA)}^3}\right]^b \times \left[\frac{F'(\mathrm{Sa})}{(\mathrm{SA})^2}\right]^c\left[\frac{\mathrm{St}F'}{(\mathrm{SA})^3}\right]^d\left[\frac{\Delta T}{(T' - T_g)}\right]^e\left[\frac{S}{M_o}\right]^f \quad (15)$$

Or $X = KA^aB^bC^cD^dE^eN^f$. Taking a logarithm on both sides,

$$\log X = \log K + a\log A + b\log B + c\log C + \mathrm{d}\log D + e\log E + f\log N \quad (16)$$

where

$$X = \frac{q}{\mathrm{Hy}}, \quad A = \frac{(T' - T_g)\lambda}{\mathrm{Hy(SA)}^2}$$

$$B = \frac{(T' - T_g)C_pF'\nu}{\mathrm{Hy(SA)}^3}, \quad C = \frac{F'\mathrm{Sa}}{(\mathrm{SA})^2}$$

$$D = \frac{F'\mathrm{St}}{(\mathrm{SA})^3}, \quad E = \frac{\Delta T}{(T' - T_g)}, \quad N = \frac{S}{M_o} \quad (17)$$

There are seven unknown exponents in eq. (16) to be determined in order to find out the rate of heat generation. For this purpose, values of X, A, B, C, D, E, and N are evaluated by putting the experimental value of q, Hy, $(T' - T_g)$, ν, SA, C_p, F', Sa, St, λ, ΔT, S, and M_o. These are reported in Tables IV and V for SBR and NR vulcanizates, respectively. The measurements were done under the conditions of the heat buildup experiments, as discussed in the Experimental section.

The same expression for heat generation of rubber was also obtained by using Rayleigh's method.

Equations are now developed by putting the values of $\log X$, $\log A$, $\log B$, $\log C$, $\log D$, $\log E$, and $\log N$, which are obtained by putting the experimental value of q, Hy, $(T' - T_g)$, ν, SA, C_p, F', Sa, St, λ, ΔT, S, and M_o. The equations are

$$X_{11} = \log K + A_{11}a + B_{11}b + C_{11}c + \mathrm{D}_{11}d + E_{11}e + N_{11}f$$

$$\cdots\cdots\cdots\cdots\cdots\cdots\cdots\cdots\cdots\cdots\cdots\cdots\cdots\cdots\cdots\cdots$$

$$\cdots\cdots\cdots\cdots\cdots\cdots\cdots\cdots\cdots\cdots\cdots\cdots\cdots\cdots\cdots\cdots$$

$$X_{77} = \log K + A_{77}a + B_{77}b + C_{77}c + \mathrm{D}_{77}d + E_{77}F + N_{77}f$$

More concisely, we can write the above equation as

$$\sum_{i=1}^{7} X_{ii} = \sum_{i=1}^{7} \log K + A_{ii}a + B_{ii}b + \mathrm{C}_{ii}c + D_{ii}d + E_{ii}e + N_{ii}f$$

Now we apply $[W]\{Y\} = \{Z\}$, where

$$W = \begin{bmatrix} 1 & A_{11} & B_{11} & C_{11} & D_{11} & E_{11} & N_{11} \\ 1 & A_{22} & B_{22} & C_{22} & D_{22} & E_{22} & N_{22} \\ 1 & A_{33} & B_{33} & C_{33} & D_{33} & E_{33} & N_{33} \\ 1 & A_{44} & B_{44} & C_{44} & D_{44} & E_{44} & N_{44} \\ 1 & A_{55} & B_{55} & C_{55} & D_{55} & E_{55} & N_{55} \\ 1 & A_{66} & B_{66} & C_{66} & D_{66} & E_{66} & N_{66} \\ 1 & A_{77} & B_{77} & C_{77} & D_{77} & E_{77} & N_{77} \end{bmatrix}_{7\times 7}$$

W is a square matrix with

$$W = \begin{vmatrix} 1 & A_{11} & B_{11} & C_{11} & D_{11} & E_{11} & N_{11} \\ \cdots & \cdots & \cdots & \cdots & \cdots & \cdots & \cdots \\ \cdots & \cdots & \cdots & \cdots & \cdots & \cdots & \cdots \\ 1 & A_{77} & B_{77} & C_{77} & D_{77} & E_{77} & N_{77} \end{vmatrix} \neq 0$$

$$\{Y\} = \begin{Bmatrix} \log k \\ a \\ b \\ c \\ d \\ e \\ f \end{Bmatrix} = \text{column matrix}$$

$$\{Z\} = \begin{Bmatrix} \log X_{11} \\ \log X_{22} \\ \log X_{33} \\ \log X_{44} \\ \log X_{55} \\ \log X_{66} \\ \log X_{77} \end{Bmatrix} = \text{column matrix}$$

Now,

$$\begin{Bmatrix} \log K \\ a \\ b \\ c \\ d \\ e \\ f \end{Bmatrix} = \begin{bmatrix} 1 & A_{11} & B_{11} & C_{11} & D_{11} & E_{11} & N_{11} \\ 1 & A_{22} & B_{22} & C_{22} & D_{22} & E_{22} & N_{22} \\ 1 & A_{33} & B_{33} & C_{33} & D_{33} & E_{33} & N_{33} \\ 1 & A_{44} & B_{44} & C_{44} & D_{44} & E_{44} & N_{44} \\ 1 & A_{55} & B_{55} & C_{55} & D_{55} & E_{55} & N_{55} \\ 1 & A_{66} & B_{66} & C_{66} & D_{66} & E_{66} & N_{66} \\ 1 & A_{77} & B_{77} & C_{77} & D_{77} & E_{77} & N_{77} \end{bmatrix}^{-1} \times \begin{Bmatrix} \log X_{11} \\ \log X_{22} \\ \log X_{33} \\ \log X_{44} \\ \log X_{55} \\ \log X_{66} \\ \log X_{77} \end{Bmatrix}$$

Hence,

$$\begin{Bmatrix} \log K \\ a \\ b \\ c \\ d \\ e \\ f \end{Bmatrix} = \begin{Bmatrix} K' \\ a' \\ b' \\ c' \\ d' \\ e' \\ f' \end{Bmatrix}$$

Using the experimental results at 50°C of SBR compounds filled with 30, 40, and 50 phr carbon black and those at 32°C for compounds loaded with 30, 50, 60, and 70 phr black, the rate of heat generation per unit time per unit volume is

$$q = 6.221\ 10^{-29}(\mathrm{Sa})^{+4.619}(F')^{+0.571}(\mathrm{Hy})^{+0.525} \times (\mathrm{SA})^{+3.590}(S)^{+0.566}(\nu)^{+0.817}(T' - T_g)^{-0.639} \times (\Delta T)^{+1.114}(M_o)^{-0.566}(\mathrm{St})^{-4.865} \times (\lambda)^{-0.342}(C_p)^{+0.817} \quad (18)$$

For NR compounds the same expression is obtained using the data of Table V. Hence, the above relationship is true for filled NR and SBR vulcanizates.

Table V Physical Properties of NR Compounds

Properties/ Mix Number	B_0	B_{20}	B_{30}	B_{40}	B_{50}	B_{60}	B_{70}	C_{50}^{10}	C_{50}^{20}	D_{50}^{10}	F_4
Hysteresis loss at (J m^3 s)E-06											
32°C	0.08	0.39	0.68	1.03	1.56	2.47	3.57	1.73	2.00	1.86	3.67
50°C	0.07	0.29	0.56	0.84	1.33	2.05	2.74	1.57	1.67	1.60	2.85
Young's modulus at (MPa)											
32°C	1.33	2.33	3.05	4.44	5.00	6.20	7.40	6.00	6.66	7.00	8.90
50°C	1.00	1.90	2.70	3.30	4.40	5.60	6.50	5.00	5.60	6.00	8.00
Rate of temperature rise at (K/s)											
32°C	0.05	0.06	0.07	0.09	0.12	0.13	0.15	0.11	0.10	0.11	0.10
50°C	0.03	0.05	0.06	0.07	0.10	0.11	0.13	0.10	0.08	0.09	0.08
Thermal conductivity at 32°C and 50°C (W m K)	0.175	0.222	0.240	0.250	0.253	0.255	0.257	0.253	0.253	0.255	0.255
Specific heat at (J kg K)											
32°C	1921	1980	2680	1560	1317	1637	1098	980	1349	638	1113
50°C	1980	2230	2769	1563	1364	1664	1129	1044	1396	699	1131
$(T' - T_g)$ (K) at											
32°C	66	63	63	62	62	62	61	61	61	61	58
50°C	84	81	81	80	80	80	79	79	79	79	76

Structure of the filler: 114 cm^3 DBP absorption/100 g; surface area of the filler: 120 m^2 N_2/g; stress on the sample during measurement of heat generation: 0.999 MPa; frequency during measurement of heat generation: 30 Hz; stroke, i.e., amplitude of deformation: 4.45 E-03 m; temperature difference between wall and environment: 1 K; cross-sectional area of the heat build-up sample: 2.488 E-04 m^2. Hysteresis loss was measured under compression and converted to 30 Hz by using the universal WLF equation.[3]

Discussion on Model Heat Generation Equation

It is observed from the model heat generation equation that the heat generation increases with an increase of hysteresis loss, frequency, filler loading, stroke, temperature difference between the wall and the environment, surface area, and stress. However, this decreases with an increase of modulus, $(T' - T_g)$, and thermal conductivity. All these are in agreement with conventional theory, literature results, and our experimental observations as discussed below.

Surface Area of Filler

At constant loading the surface area of carbon black increases with decreasing particle size, resulting in the increasing tendency to form a secondary network. The breakdown of these secondary structures during deformation increases with an increase of surface area. As a result hysteresis loss increases, leading to higher heat generation in a rubber compound. Thermal conductivity is also important in this case. Higher thermal conductivity lowers the heat generation in a rubber compound. Our model equation developed here indicates that the rate of increase of heat generation increases with an increase of surface area to the power of 4.619.

Filler Loading

When carbon black is mixed with rubber, the first step is the random dispersion of the black into the rubber matrix followed by the penetration of the rubber into the void space replacing trapped air and eliminating loose black. There are formations of networks throughout the rubber matrix. This network, which increases with an increase of filler loading, breaks down during the deformation of the sample. Hysteresis loss increases with an increase of breakdown of this network. As a result, heat generation in a rubber compound increases. Another factor, thermal conductivity, also plays an important role. Heat generation will decrease

with an increase of thermal conductivity. In this case two opposite factors act simultaneously. The former is the dominant factor during the variation of filler loading in the rubber matrix. This is also indicated in our model equation. The rate of increase of heat generation with filler loading is 0.571.

Hysteresis Loss

There are always some irreversible processes during deformation of rubber vulcanizates that lead to the conversion of mechanical energy into heat. Stress–strain curves under tension or compression and subsequent retraction generate a hysteresis loop. Hysteresis loss is the ratio of the rate dependence or viscous component to the elastic component of the deformation energy. It is also a measure of deformation energy that is not stored but is converted into heat. So, the rate of heat generation is expected to increase with an increase of hysteresis loss as observed in some samples in Tables IV and V. This is predicted in our model equation. The exponent of the hysteresis loss in the equation is 0.525. Deviation from this prediction for the resin filled sample, the samples having different types of black, and the samples containing higher concentration of sulfur and accelerator simply indicates that other parameters shown in eq. (18) override the hysteresis loss.

Stroke, Stress, and Frequency

Stroke is an important parameter in the heat generation of rubber. An experiment may be considered in which a filled vulcanizate is subjected at constant frequency to a periodic sinusoidal stroke, the SA being increased stepwise. As the filled rubber matrix contains primary and secondary agglomerate structures, an increase in the stroke will break down the structure of the black. In the lower stroke amplitude, the storage modulus remains intact. However, at higher stroke amplitude the secondary agglomerate structures are destroyed with an increase of SA, leading to a decrease of the storage modulus. So, the heat generation increases. Increase in stress or frequency will have a similar influence on the heat generation. Our data for NR and SBR systems reported in Tables IV and V are in line with this prediction. These are also confirmed from our model equation. The rate of increase of heat generation with increase of stroke amplitude is 3.59, with increase of frequency 0.817, and with increase of stress 0.566.

Difference Between Application and Glass Transition Temperatures ($T' - T_g$)

The monomeric friction coefficient is the frictional force per unit velocity encountered by a monomer unit of the macromolecules as it pushes its way through its surroundings. The surroundings consist of other macromolecules, but their average resistance can be reckoned as a force per unit velocity. The monomeric friction coefficient (β) decreases rapidly with increasing temperature. As a result, the rate of heat generation will be decreased with an increase of temperature. The glass transition temperature of carbon black filled rubber is raised typically by only 2–3°C.[9] If we increase ($T' - T_g$) at constant T_g, the rate of heat generation will be decreased in agreement with our model equation. The rate of decrease of heat generation with increase of ($T' - T_g$) is 0.639.

Temperature Difference Between Wall and Environment

The temperature difference between the wall of the rubber and the environment of the rubber surface is important in heat generation of rubber. There will be heat loss in the case of a temperature difference between the wall and the environment. The coefficient of friction between molecules increases due to the decrease of mobility of the molecules. During deformation of the rubber sample, the heat generation will be further increased. So the rate of heat generation will increase with an increase of temperature difference between the wall and the environment. This is also indicated in our model equation. The rate of increase of heat generation with an increase of temperature difference between the wall and the environment is 1.114.

Modulus

Modulus is an important factor in a rubber compound. Modulus arises either from the permanent chemical crosslinks or from mobile physical crosslinks. Additional crosslinks apparently introduced into the matrix by reinforcing fillers are different from the chemical crosslinks. The model equation derived predicts that the exponent of modulus is −0.566.

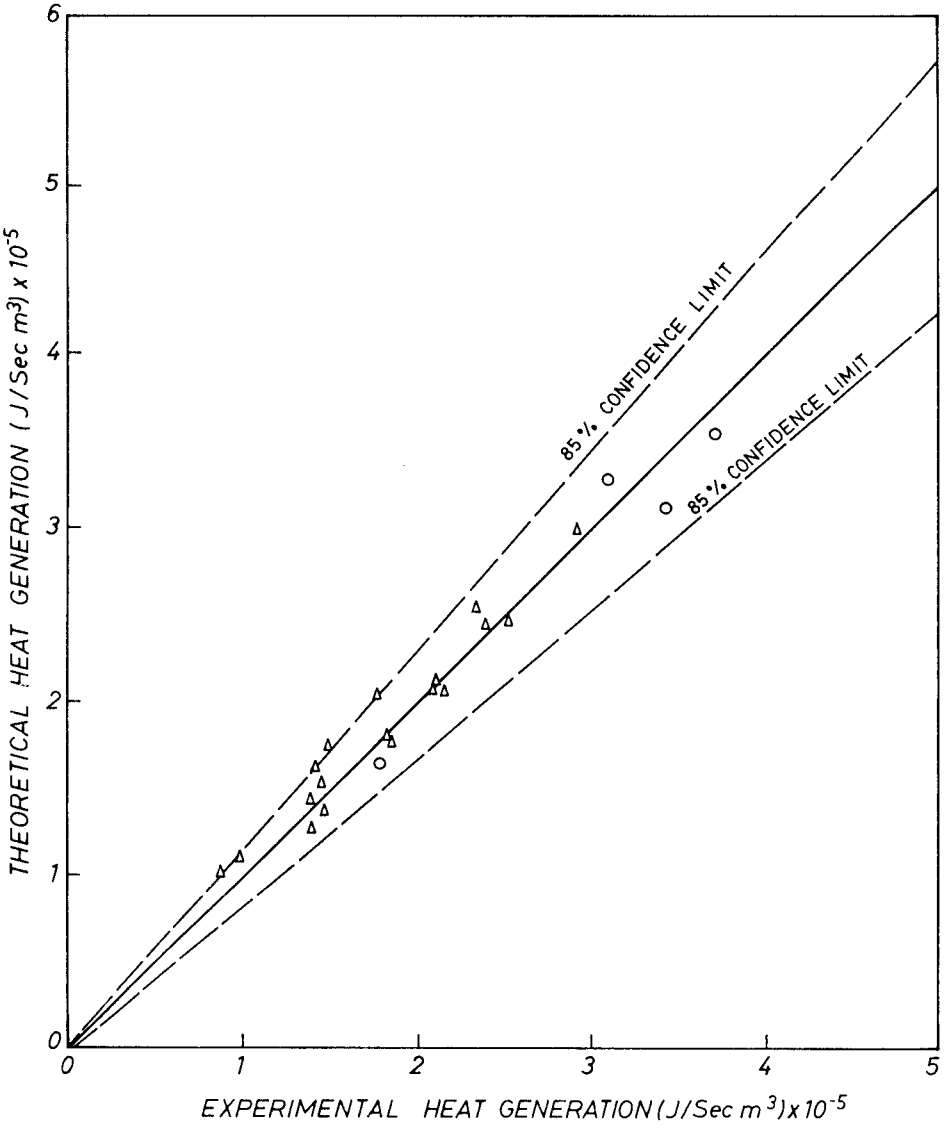

Figure 10 Experimental heat generation as a function of theoretical heat generation for (○) filled natural rubber vulcanizates and (△) filled styrene–butadiene rubber vulcanizates.

Structure of Black

A literature survey indicates contradictory reports on the influence of carbon black structure on heat generation. Heat generation will increase,[22] have a small increase,[23] be unaffected,[24] or will decrease[24] with an increase of structure. But the model equation predicts that the heat generation decreases with an increase of structure. This can be explained as follows. Increasing structure is associated with a change in hysteresis loss, modulus, and thermal conductivity. Although the hysteresis loss will increase with increasing structure, the modulus and the thermal conductivity are expected to increase. The balancing effects of these factors would determine the rate of heat generation. The exponent is determined to be −4.865.

Thermal Conductivity and Specific Heat

Thermal conductivity increases with an increase of carbon black loading due to the larger extensive network structures. The type of network configuration depends on the nature of the elastomer and also on the compounding ingredients. Again, conductivity decreases with an increase of tempera-

ture.[12] Specific heat also increases with an increase of temperature as observed by Furukawa and Reilly.[25] Tables IV and V indicate that the specific heat increases with an increase of temperature in NR and SBR. The model equation shows that the rate of heat generation increases with an increase of specific heat and decrease of thermal conductivity. These are in agreement with our conventional theory. In the model equation, the rate of heat generation is proportional to the power of 0.817 with respect to specific heat and −0.342 with respect to thermal conductivity.

From the above discussion it is apparent that the model heat generation equation explains the contradictory results in the case of resin loadings, type of black loadings, and higher concentration of sulfur and accelerator. Decrease of heat generation with increase of hysteresis loss may be due to the increase of modulus in vulcanizates containing resin and a higher degree of sulfur and accelerator. An increase of heat generation with a decrease of hysteresis loss at constant modulus may be due to the increase of surface area in the case studies of black variations.

Using the experimental data at 32°C of 20 and 40 phr black filled SBR and those at 50°C of SBR containing 20, 60, and 70 phr black from Table III and eq. (18), the theoretical heat generation was calculated. [These data were not used earlier for deriving eq. (18)]. The data are now plotted against the experimental value of heat generation. Such a plot is shown in Figure 10. It is observed that the slope of this line is one. The theoretical and experimental values of heat generation for NR vulcanizates are now plotted on the same curve. It is interesting to note that all the data lie on the same line within an error of ±15%. Hence, the equation derived above seems to be universal in nature and independent of the nature of rubber, filler, resin, and other compounding ingredients. To test this equation further, heat generation experiments were carried out at four different stress levels and three different stroke levels. The rate of heat generation data are plotted against stress and stroke in Figures 11 and 12. It is observed that the heat generation increases with both stress and stroke. A line with a slope of 0.6 in the case of stress and a line with a slope of 3.6 in the case of stroke satisfy the experimental data and are in good accord with the predictions made in eq. (18).

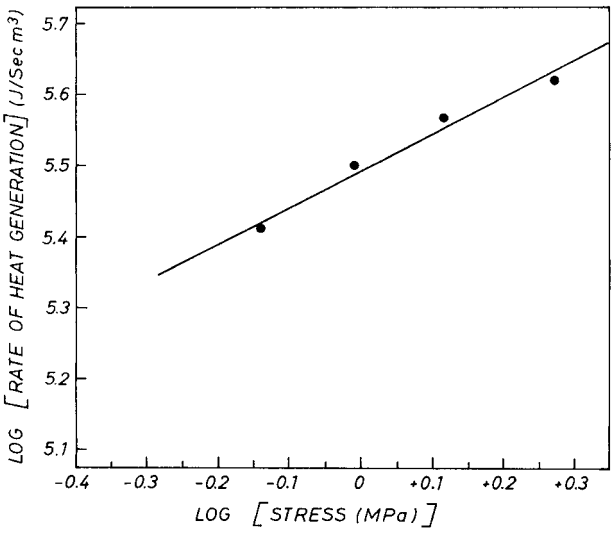

Figure 11 Logarithmic plot of heat generation versus stress in a heat buildup experiment for SBR compounds containing 70 phr black at 50°C and stroke of 4.45 E-03 m.

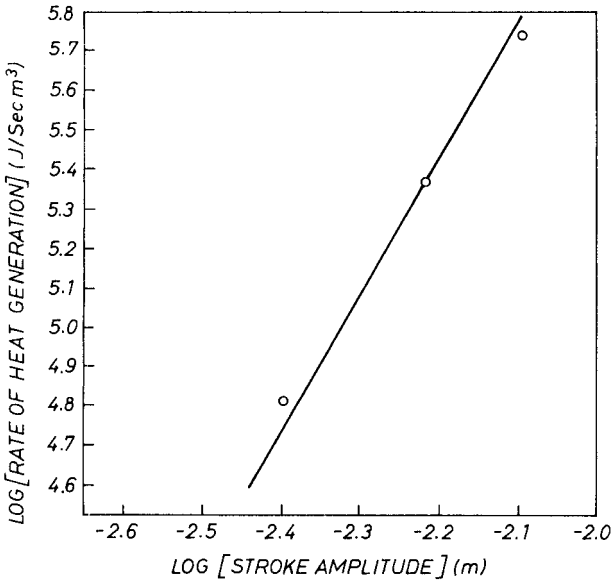

Figure 12 Logarithmic plot of heat generation versus stroke amplitude in a heat buildup experiment for SBR vulcanizates containing 70 phr black at 50°C and a load of 0.999 MPa.

CONCLUSIONS

The aim of this research was to investigate the factors responsible for heat generation in NR and SBR vulcanizates. A relationship relating heat generation with the operating conditions and the material properties of rubber was developed by using the Buckingham π theorem and Rayleigh's

method. The following observations and conclusions are made.

Heat generation in a rubber compound not only depends on the hysteresis loss but is also a nonlinear function of other parameters as follows:

$$q = 6.221\ 10^{-29}(\mathrm{Sa})^{+4.619}(F')^{+0.571}(\mathrm{Hy})^{+0.525} \times (\mathrm{SA})^{+3.590}(S)^{+0.566}(\nu)^{+0.817}(T' - T_g)^{-0.639} \times (\Delta T)^{+1.114}(M_o)^{-0.566}(\mathrm{St})^{-4.865} \times (\lambda)^{-0.342}(C_p)^{+0.817}$$

It increases with the increase of hysteresis loss, frequency, specific heat, stress, stroke amplitude, filler loading, surface area of filler, and the temperature difference between the wall and the environment. The heat generation decreases with an increase of $(T' - T_g)$, thermal conductivity, and structure of the black. The model equation explains the contradictory results of a decrease of heat generation with an increase of hysteresis loss by an increase of modulus. This explains the abnormal result of the increase of heat generation at constant modulus and loading of filler by an increase of surface area of the filler. This was found to quantitatively predict the amount of heat generation of a few unknown SBR and NR vulcanizates. The model equation is also verified by varying the stress and stroke amplitude in the heat generation experiment and shows good accord with the predictions made in eq. (18).

The authors acknowledge the financial support provided by DRDO, New Delhi, for carrying out this research work.

REFERENCES

1. G. Rodriguez, paper presented at the 133th meeting of the Rubber Division, American Chemical Society, Dallas, TX, April 1988.
2. P. Kainradl and G. Kaufman, *Rubber Chem. Technol.,* **49,** 823 (1976).
3. J. D. Ferry, in *Viscoelastic Properties of Polymers,* 3rd ed., Wiley, New York, 1980, p. 80.
4. J. E. Mark, B. Erman, and F. R. Eirich, in *Science and Technology of Rubber,* 2nd ed., Academic Press, London, 1994, p. 235.
5. S. D. Gehman, *Rubber Chem. Technol.,* **30,** 1202 (1947).
6. J. H. Dillan and S. D. Gehman, *Rubber Chem. Technol.,* **20,** 827 (1947).
7. L. S. Priss, *Kautsch. Gummi Kunstst.,* **19,** 639 (1966).
8. E. Meinecke, *Rubber Chem. Technol.,* **64,** 269 (1991).
9. A. I. Medalia, *Rubber Chem. Technol.,* **51,** 437 (1978).
10. A. N. Gent and M. Hindi, *Rubber Chem. Technol.,* **61,** 892 (1988).
11. D. Hands and F. Forsfall, *Rubber Chem. Technol.,* **50,** 253 (1977).
12. A. K. Sircar and J. L. Wells, *Rubber Chem. Technol.,* **55,** 191 (1982).
13. M. P. Wagner, *Rubber Chem. Technol.,* **49,** 697 (1976).
14. M. P. Wagner, *Rubber Chem. Technol.,* **47,** 697 (1974).
15. S. Wolff, paper presented at the 131st meeting of the Rubber Division, American Chemical Society, New York, April 8–11, 1986.
16. T. K. Bhowmick, A. K. Bhowmick, and B. R. Gupta, *Plast. Rubber Process. Appl.,* **7,** 1 (1987).
17. M. K. Kar and S. Bahadur, *Wear,* **30,** 337 (1974).
18. N. Viswanath and D. G. Below, *Wear,* **42,** 181 (1995).
19. H. L. Langharr, *Dimensional Analysis and Theory of Models,* Wiley, New York, 1951.
20. J. G. Khudsen and D. L. Katz, *Fluid Mechanics and Heat Transfer,* McGraw–Hill, New York, 1958.
21. W. L. McCabe, J. C. Smith, and P. Harriott, *Unit Operation in Chemical Engineering,* McGraw–Hill, New York, 1985.
22. D. T. Norman, in *The Vanderbilt Rubber Handbook,* 13th ed., Robert F. Ohm, Ed., RT Vanderbilt Company Inc., New York, 1990, p. 420.
23. J. B. Horn, in *Rubber Technology and Manufacture,* 2nd ed., C. M. Blow, Ed., Butterworth Scientific Press, London, 1982, p. 216.
24. J. T. Byers in *Rubber Technology,* 2nd ed., M. Morton, Ed., Van Nostrand Reinhold Company, New York, 1973, p. 81.
25. G. T. Furukawa and M. L. Reilly, *J. Res. Natl. Bur. Stand.,* **56,** 285 (1956).